

# ADAMUON: ADAPTIVE MUON OPTIMIZER

**Chongjie Si<sup>1</sup>, Debing Zhang<sup>2</sup>, Wei Shen<sup>1\*</sup>**

<sup>1</sup>MoE Key Lab of Artificial Intelligence, AI Institute, School of Computer Science, Shanghai Jiao Tong University. <sup>2</sup>Xiaohongshu Inc.

chongjiesi@sjtu.edu.cn

wei.shen@sjtu.edu.cn

## ABSTRACT

We propose AdaMuon, a novel optimizer that combines element-wise adaptivity with orthogonal updates for large-scale neural network training. AdaMuon incorporates two tightly coupled mechanisms: (1) an element-wise second momentum estimator applied to orthogonalized update directions, and (2) a sign-stabilized orthogonal update, where the momentum is first sign-transformed before orthogonalization. These two components jointly enable variance-adaptive scaling while maintaining stable update geometry. In addition, AdaMuon employs an RMS-aligned rescaling strategy to match the root-mean-square update magnitude to Adam, allowing direct reuse of existing learning rate schedules without extra tuning. Experiments demonstrate that AdaMuon not only maintains stability but can surpass Adam by more than 40% training efficiency in large-scale scenarios.

## 1 INTRODUCTION

Optimization algorithms are a cornerstone of modern deep learning, directly shaping training dynamics and influencing both convergence speed and generalization performance. As model scales have grown to billions or even trillions of parameters (Brown et al., 2020; Chowdhery et al., 2023; Touvron et al., 2023; Liu et al., 2024; Moonshot, 2025), optimizers face increasingly heterogeneous gradient landscapes and complex parameter geometries. Adaptive methods (Duchi et al., 2011; Tieleman, 2012; Loshchilov & Hutter, 2017), exemplified by Adam (Kingma & Ba, 2014), have become the de facto choice for large-scale training owing to their variance-based step size control and ease of tuning. However, over a decade after its introduction, the field is witnessing a growing demand for a new generation of optimizers that are better aligned with the computational and statistical challenges of training modern large foundation models.

Muon (Jordan et al., 2024) has been introduced as a representative of this emerging direction. It applies polar decomposition to transform raw momentum matrices into spectrally normalized, direction-only updates. This orthogonalization yields improved stability for large-scale two-dimensional parameter blocks such as transformer weight matrices (Liu et al., 2025; Shah et al., 2025; Chen et al., 2025; Tveit et al., 2025), and has already been deployed in ultra-scale training, including GLM-4.5 (Zeng et al., 2025) with 355B parameters and KIMI Moonshot (Moonshot, 2025) with over 1T parameters. It is widely regarded as a strong candidate for the next-generation optimizer that could potentially replace Adam in large-scale model training.

Building on this momentum, we aim to push the boundary of optimizers toward a paradigm that not only preserves the well-conditioned, geometry-aware updates of Muon but also adapts to the diverse statistical characteristics of individual coordinates—combining the efficiency of first-order methods with the robustness of second-order adaptivity. This motivation leads us to propose AdaMuon, an initial step toward this vision. AdaMuon incorporates element-wise variance adaptation into orthogonal updates through two tightly coupled mechanisms: an element-wise second momentum estimator applied after orthogonalization, and a sign-stabilized orthogonal update. Together with an RMS-aligned rescaling strategy for seamless integration with existing learning rate schedules, these components enable AdaMuon to unify matrix-level stability and coordinate-wise adaptivity, offering a principled path toward the next generation of large-scale optimizers. Experiments show

---

\*Corresponding author.

that AdaMuon not only achieves stable convergence but also improves training efficiency by more than 40% compared to Adam in large-scale scenarios.

In the remainder of this paper, Sec. 2 reviews Muon and its extensions, along with the necessity and challenges of incorporating second momentum estimation; Sec. 3 presents the AdaMuon algorithm in detail; and Sec. 4 demonstrates that AdaMuon consistently outperforms other methods across a variety of models and datasets. Overall, we show that AdaMuon is a versatile algorithm that scales effectively to large-scale models.

---

**Algorithm 1** The AdaMuon Optimizer

---

**Input:** Initial 2D-weights  $\mathbf{W}_0 \in \mathbb{R}^{n \times m}$ , loss function  $\mathcal{L}$ , learning rate  $\eta$ , weight decay  $\lambda$ , momentum  $\beta$ , Newton–Schulz steps  $T$ , small constant  $\varepsilon$   
**Output:** Updated weights  $\mathbf{W}$   
Initialize first-momentum  $\mathbf{M}_0 \leftarrow \mathbf{0}$ , second-momentum  $\mathbf{V}_0 \leftarrow \mathbf{0}$   
**for** each iteration  $t = 1, 2, \dots$  **do**  
  Compute gradient:  $\mathbf{G}_t = \nabla_{\mathbf{W}_t} \mathcal{L}(\mathbf{W}_t)$   
  Update first momentum:  $\mathbf{M}_t = \beta \cdot \mathbf{M}_{t-1} + \mathbf{G}_t$   
  Compute sign-stabilized orthogonal direction:  $\mathbf{O}_t = \text{Newton-Schulz}(\text{Sign}(\mathbf{M}_t), T)$   
  Update second momentum:  $\mathbf{V}_t = \beta \cdot \mathbf{V}_{t-1} + (1 - \beta) \cdot \mathbf{O}_t \odot \mathbf{O}_t$   
  Apply second momentum update:  $\hat{\mathbf{O}}_t = \mathbf{O}_t \oslash (\sqrt{\mathbf{V}_t} + \varepsilon \cdot \mathbf{1})$ .  
  RMS-aligned:  $\gamma_t = 0.2 \cdot \sqrt{mn} / \|\hat{\mathbf{O}}_t\|_F$   
  Update weights:  $\mathbf{W}_{t+1} = \mathbf{W}_t - \eta(\gamma_t \hat{\mathbf{O}}_t + \lambda \mathbf{W}_t)$   
**end for**

---

## 2 PRELIMINARY

### 2.1 MUON OPTIMIZER

Muon (Jordan et al., 2024) is a recently proposed optimization method designed for parameter tensors that can be represented as matrices. At iteration  $t$ , given the current weight matrix  $\mathbf{W}_t \in \mathbb{R}^{n \times m}$  and its gradient  $\mathbf{G}_t$ , momentum  $\beta$ , and learning rate  $\eta$ , Muon updates parameters according to

$$\begin{aligned} \mathbf{M}_t &= \beta \mathbf{M}_{t-1} + \mathbf{G}_t, \\ \mathbf{O}_t &= \text{Newton-Schulz}(\mathbf{M}_t, T), \\ \mathbf{W}_{t+1} &= \mathbf{W}_t - \eta \mathbf{O}_t. \end{aligned} \tag{1}$$

where  $\mathbf{M}_t$  denotes the momentum buffer at step  $t$ , initialized as a zero matrix for  $t = 0$ . The Newton–Schulz step (Bernstein & Newhouse, 2024) approximates the polar decomposition  $\mathbf{O}_t$  of  $\mathbf{M}_t$ , which corresponds to  $\mathbf{O}_t = \mathbf{U}\mathbf{V}^\top$  in the singular value decomposition (SVD)  $\mathbf{M}_t = \mathbf{U}\mathbf{S}\mathbf{V}^\top$ .  $T$  in Eq. (1) denotes the number of iteration steps. This approximation avoids the high computational cost of a full SVD, and preserves the update direction while removing anisotropic scaling.

Specifically, Newton-Schulz step begins by normalizing the momentum matrix:  $\mathbf{X}_0 = \frac{\mathbf{M}_t}{\|\mathbf{M}_t\|_F}$ . Then, for each iteration  $k$ ,  $\mathbf{X}_k$  is updated from  $\mathbf{X}_{k-1}$  as

$$\mathbf{X}_k = a\mathbf{X}_{k-1} + b(\mathbf{X}_{k-1}\mathbf{X}_{k-1}^\top)\mathbf{X}_{k-1} + c(\mathbf{X}_{k-1}\mathbf{X}_{k-1}^\top)^2\mathbf{X}_{k-1}, \tag{2}$$

where  $a$ ,  $b$ , and  $c$  are iteration coefficients, and  $\mathbf{X}_T$  is the output after  $T$  steps. Convergence requires tuning  $a$ ,  $b$ , and  $c$  so that the polynomial  $f(x) = ax + bx^3 + cx^5$  has a fixed point close to 1. Following Jordan et al. (2024), we adopt  $a = 3.4445$ ,  $b = -4.7750$ ,  $c = 2.0315$ , and  $T = 5$ , which accelerate convergence for small singular values while maintaining stability.

### 2.2 SCALING UP FOR MUON

In practice for scaling up, Muon faces two practical challenges. First, the root-mean-square (RMS) magnitude of the weight matrices can become excessively large, exceeding the high-precision range of bf16, which is harmful. Second, Muon is applied only to two-dimensional parameters (e.g., weight matrices), while one-dimensional parameters (e.g., biases) are still optimized with Adam, necessitating separate learning rates and tuning complexity into existing pipelines.

To address both issues, Liu et al. (2025) propose to control the RMS of Muon’s weights via weight decay, and introducing a scaling factor  $\gamma = 0.2\sqrt{\max(m, n)}$  to match the RMS norm of Muon’s updates to that of Adam, thereby enabling a unified learning rate schedule. The resulting update rule is

$$\mathbf{W}_{t+1} = \mathbf{W}_t - \eta \cdot (\gamma \mathbf{O}_t + \lambda \mathbf{W}_t), \quad (3)$$

where  $\lambda$  is the weight decay coefficient. This simple yet effective adjustment stabilizes the training process while enabling Muon and Adam to share the same learning rate schedule, thereby allowing seamless integration into existing optimization pipelines.

## 2.3 SECOND-MOMENTUM IN MUON: NECESSITY AND CHALLENGES

### 2.3.1 NECESSITY

Newton’s method leverages curvature via the inverse Hessian to obtain locally optimal update directions, but for large-scale models this is impractical. Adaptive optimizers such as Adam and RMSProp approximate curvature through exponential moving averages of squared gradients, enabling variance-based step size adjustment. Similarly, Muon’s polar decomposition inherently captures matrix-level second-order structure. From

$$\mathbf{O}_t = (\mathbf{M}_t \mathbf{M}_t^\top)^{-1/2} \mathbf{M}_t = \mathbf{M}_t (\mathbf{M}_t^\top \mathbf{M}_t)^{-1/2}, \quad (4)$$

it follows that Muon, like Shampoo (Gupta et al., 2018), encodes row–column second-order interactions without explicitly storing full covariance matrices.

However, this global orthogonalization does not model the local variance structure of individual parameters. In real-world training, gradient distributions are often highly anisotropic at the element level—some entries exhibit large fluctuations, while others remain consistently stable. Applying a uniform update magnitude in such cases risks overshooting in noisy coordinates and under-updating informative but low-variance ones. This mismatch might slow convergence, reduce stability, and limit Muon’s effectiveness in tasks with heterogeneous gradient statistics.

### 2.3.2 CHALLENGES

To this end, we consider integrating element-wise second-momentum estimation into Muon. The most straightforward idea is to extend Muon by directly appending a second momentum accumulator, and then scaling the orthogonal update  $\mathbf{O}_t$  with its variance estimate. However, this introduces two key design challenges:

- **First, determining which component to accumulate.** In Adam, the second momentum is naturally accumulated on the raw gradient  $\mathbf{G}_t$ , but in Muon the update direction  $\mathbf{O}_t$  is obtained through polar decomposition of the momentum buffer  $\mathbf{M}_t$ . It remains unclear whether variance tracking should be applied to  $\mathbf{G}_t$ ,  $\mathbf{M}_t$ , or  $\mathbf{O}_t$ , since each choice leads to different stability and normalization behaviors.
- **Second, achieving a normalization effect comparable to Adam.** In Adam, both the first and second moments are computed from the same gradient signal, making their ratio an effective per-element normalization of step size. In Muon, however,  $\mathbf{M}_t$  may fluctuate substantially during the early and middle stages of training, causing the resulting  $\mathbf{O}_t$  to also vary dramatically across coordinates. Consequently, no matter whether the second momentum is accumulated on  $\mathbf{G}_t$ ,  $\mathbf{M}_t$ , or  $\mathbf{O}_t$ , the resulting statistics remain unstable and fail to provide a reliable normalization effect, even potentially amplifying noise.

A careful resolution of these challenges is essential to seamlessly integrate variance adaptivity into Muon without undermining its orthogonalization benefits or its inherent scale-invariant properties.

## 3 ADAMUON

To address the aforementioned challenges, in this section, we introduce **AdaMuon**, a novel optimizer that retains the advantages of Muon’s orthogonal updates while automatically adjusting the scaling of individual elements. AdaMuon integrates two complementary mechanisms, **element-wise second momentum estimation and sign-stabilized orthogonal updates**, to simultaneously capture accurate second momentum statistics and normalize the update magnitude.

### 3.1 ELEMENT-WISE SECOND MOMENTUM ESTIMATION

To address the first challenge, we choose to accumulate the second-momentum term on  $\mathbf{O}_t$ , rather than on the raw gradient  $\mathbf{G}_t$  or the momentum buffer  $\mathbf{M}_t$ . This design is principled for two reasons. First, the raw gradient  $\mathbf{G}_t$  carries ill-conditioned scaling and directional noise that Muon’s polar decomposition is specifically designed to eliminate, making it unsuitable for stable variance tracking. Second, while  $\mathbf{M}_t$  provides a temporally smoothed gradient, it remains unstable at the element level during the early and middle stages of training. Moreover, since the final update direction is derived from  $\mathbf{O}_t$ , accumulating variance on  $\mathbf{M}_t$  introduces a mismatch with the rescaling basis used in the update. In contrast,  $\mathbf{O}_t$  provides a geometrically normalized and stable descent direction, offering a cleaner basis for variance estimation.

Formally, let  $\mathbf{O}_t$  denote the orthogonalized update matrix obtained via Newton–Schulz iteration. We maintain an exponential moving average of its element-wise squared values:

$$\mathbf{V}_t = \beta \cdot \mathbf{V}_{t-1} + (1 - \beta) \cdot \mathbf{O}_t \odot \mathbf{O}_t, \quad (5)$$

where  $\odot$  denotes Hadamard product. Here,  $\mathbf{V}_t$  serves as the second momentum buffer for the orthogonalized update, analogous to the variance accumulator in Adam. The coefficient  $\beta$  is inherited directly from Muon’s momentum parameter, ensuring that AdaMuon does not introduce any additional hyper-parameters. The variance-normalized update direction is then obtained as

$$\hat{\mathbf{O}}_t = \mathbf{O}_t \oslash (\sqrt{\mathbf{V}_t} + \varepsilon \cdot \mathbf{1}), \quad (6)$$

where  $\oslash$  denotes element-wise division,  $\sqrt{\mathbf{V}_t}$  represents the element-wise square root of the variance estimates,  $\mathbf{1}$  is an all-ones matrix of the same shape as  $\mathbf{O}_t$ , and  $\varepsilon$  is a small positive constant added for numerical stability. This step adaptively reweights each element of the orthogonalized direction according to its estimated variance, suppressing noisy coordinates while preserving Muon’s globally coherent update geometry.

### 3.2 STABILIZING ORTHOGONAL UPDATES VIA SIGN TRANSFORMATION

While the element-wise second-momentum estimator effectively captures variance in principle, it becomes less suitable during the early to mid stages of training. In this regime, gradients are unstable and may undergo large fluctuations, causing the momentum buffer  $\mathbf{M}_t$  itself to vary substantially at the element level. Consequently, the polar decomposition produces orthogonal updates  $\mathbf{O}_t$  that also fluctuate dramatically across coordinates. Accumulating such unstable  $\mathbf{O}_t$  into a second momentum term fails to yield meaningful normalization and may even introduce adverse effects by amplifying noise rather than stabilizing it.

We hope  $\mathbf{O}_t$  to be both usable in second momentum scaling and stable enough for variance-based normalization. To achieve this, we propose to first apply a transformation  $f$  to  $\mathbf{M}_t$ , so that

$$\mathbf{O}_t = g(f(\mathbf{M}_t)), \quad g(\cdot) = \text{polar}(\cdot). \quad (7)$$

Recall that  $g(c\mathbf{M}_t) = g(\mathbf{M}_t)$  for  $\forall c > 0$ , which indicates that  $g$  is globally scale-invariant, preserving only the overall directional information of  $\mathbf{M}_t$ . However,  $g$  alone does not stabilize element-wise fluctuations.  $f$  is therefore designed to complement  $g$ : while  $g$  enforces global directionality,  $f$  operates element-wise to preserve coordinate-level orientation while mitigating volatility.

**Theorem 1** (Characterization of admissible element-wise transformations). *Let  $f : \mathbb{R} \rightarrow \mathbb{R}$  be a function applied element-wise to  $\mathbf{M}_t$  before the polar operator  $g(\cdot) = \text{polar}(\cdot)$ . Suppose  $f$  satisfies the following conditions:*

1. (Scale invariance)  $f(cx) = f(x)$  for all  $x \in \mathbb{R}$  and  $c > 0$ .
2. (Sign consistency) For  $x \neq 0$ ,  $\text{sign}(f(x)) = \text{sign}(x)$ .
3. (Odd symmetry)  $f(-x) = -f(x)$ .
4. (Bounded range) There exists  $C < \infty$  such that  $|f(x)| \leq C$  for all  $x$ .

*Then  $f$  must be of the form  $f(x) = c \cdot \text{sign}(x)$ ,  $c > 0$ . Moreover, since  $g$  is globally scale-invariant, the multiplicative constant  $c$  is immaterial, and the unique canonical choice is  $f(x) = \text{sign}(x)$ .*

The proof of Theorem 1 is shown in Appendix. A. Condition (1) ensures that per-coordinate magnitudes do not reintroduce instability when passed into  $g$ , aligning with  $g$ ’s own scale-invariance at the global level. Conditions (2) and (3) constrain the directional behavior of  $f$ , while Condition (4) guarantees value stability. Taken together,  $f(x) = \text{sign}(x)$ , which satisfies all four desiderata. This yields a stabilized input to  $g$ , ensuring that  $\mathbf{O}_t$  remains both orthogonal and robust enough for variance-based normalization.

### 3.3 RMS-ALIGNED RESCALING

To maintain compatibility with Adam’s learning rate schedules, we scale the RMS norm of AdaMuon’s update  $\hat{\mathbf{O}}_t$  (after second momentum estimation in Eq. (6)) to match Adam’s empirical RMS value of  $\approx 0.2$  (Liu et al., 2025), yielding

$$\gamma_t = \frac{0.2}{\text{RMS}(\hat{\mathbf{O}}_t)} = \frac{0.2\sqrt{mn}}{\|\hat{\mathbf{O}}_t\|_F}. \quad (8)$$

Finally, the rescaled update is applied to the parameters as

$$\mathbf{W}_{t+1} = \mathbf{W}_t - \eta(\gamma_t \hat{\mathbf{O}}_t + \lambda \mathbf{W}_t), \quad (9)$$

The pseudo-code of AdaMuon is shown in Alg. 1. In addition, we provide further discussions on the omission of bias correction in the second momentum estimation (unlike Adam). Please refer to Appendix B for more details.

## 4 EXPERIMENT

### 4.1 EXPERIMENTAL SETUP

**Baselines.** We compare AdaMuon against AdamW (Loshchilov & Hutter, 2017) and Muon (Jordan et al., 2024). Given Muon’s strong performance in large-scale training, we consider these two baselines sufficient to demonstrate the effectiveness of AdaMuon. Since Muon operates only on matrices and applies a separate Adam optimizer for the remaining parameters, we set the learning rates of both optimizers to be the same. For AdamW, the first and second momentum coefficients are set to 0.9 and 0.95, respectively; Muon uses  $\beta = 0.95$ , and AdaMuon introduces no extra hyper-parameters. The weight decay  $\lambda$  for these optimizers are set to 0.1.

**Model Architectures.** We evaluate AdaMuon on two representative model families: GPT-2 and Qwen2.5. All GPT-2 experiments are based on the nanoGPT (Karpathy, 2022) implementation of the GPT-2 architecture (Radford et al., 2019). We consider four scales—Small (125M), Medium (355M), Large (770M), and XL (1.5B). Following the default configurations in nanoGPT, we remove bias terms in all linear layers, use the GeLU activation function, and set the dropout rate to 0.0. Two modifications are applied: (1) replacing the original learned positional embedding (WPE) with Rotary Positional Embedding (RoPE) (Su et al., 2024), and (2) substituting the cosine learning rate schedule with the warmup-stable policy. For Qwen2.5 (Qwen et al., 2025), we adopt the 1.5B dense model following the official architecture specifications.

**Datasets.** GPT-2 models are trained on the OpenWebText dataset (Gokaslan et al., 2019), which contains approximately 9B training tokens and 4.4M validation tokens, all tokenized with the standard GPT-2 tokenizer. For Qwen2.5 training, the dataset is collected from online corpora, with low-quality content removed through a combination of manually filtering rules and LLM-based quality assessment. Beyond general text, it contains high-quality code, math, and multilingual content.

**Training Details.** For GPT-2 experiments, all models are trained on approximately 49.2B training tokens for 100K steps, with a context length of 1024 and a warmup period of 2K steps. For Qwen2.5 experiments, the model is trained on 100B tokens with a context length of 8196 with 6e-4 learning rate. All the other hyper-parameters follow the respective official configurations. All other training settings including random seed, etc, unless otherwise specified, are kept consistent across methods.

**Evaluation Metric** We measure training efficiency improvement over Adam. For each method, we record the number of tokens required to reach the same training/validation loss achieved by Adam after training on  $a$  tokens. If Muon or AdaMuon requires  $b$  tokens to match this loss, the efficiency improvement is computed as  $\frac{a-b}{a} \times 100\%$ . This metric reflects the proportion of training tokens saved relative to Adam while achieving equivalent performance.

#### 4.2 RESULT

**GPT-2 Results.** Fig. 1 illustrates the loss–token curves of AdamW, Muon and AdaMuon under two learning-rate settings, and Table 1 summarizes the corresponding training efficiency of Muon and AdaMuon. Across all four GPT-2 scales, both Muon and AdaMuon deliver significant efficiency gains over AdamW, validating the benefit of geometry-preserving updates. Notably, AdaMuon consistently achieves the highest efficiency, regardless of model size or learning rate, demonstrating the effectiveness of integrating second-moment scaling with RMS-norm alignment. We also note that for GPT-2 XL with a learning rate of  $1 \times 10^{-3}$ , the efficiency gap is particularly large: in this regime, AdamW exhibits unstable training with multiple loss spikes, whereas Muon and AdaMuon remain stable, enabling them to reach the target loss substantially faster.

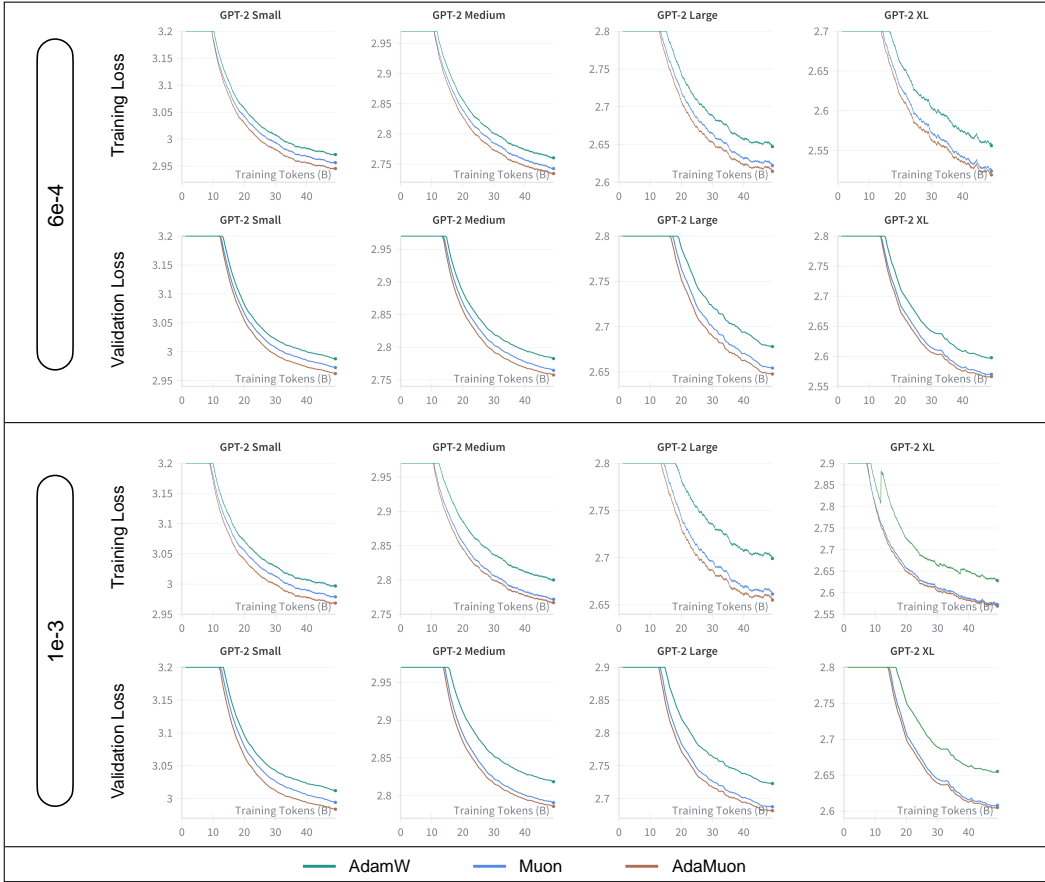


Figure 1: Training and validation loss comparisons of AdamW, Muon, and AdaMuon.

**Qwen2.5 Results.** Fig. 2 presents the training results of Qwen2.5. Consistent with the GPT-2 results, AdaMuon exhibits faster convergence than both Muon and AdamW across the entire training trajectory. In terms of time-to-target reduction, AdaMuon shortens the wall-clock time needed to reach the same loss by 30.8% compared to Adam and by 2.9% compared to Muon, translating into substantial savings in large-scale deployments. Moreover, we provide the evaluation results of Qwen2.5 after 100B-token training on 15 benchmark datasets. As reported in Table 2, models

Table 1: Training efficiency of Muon and AdaMuon over AdamW. All improvements are computed relative to the AdamW baseline (49.2B training tokens).

Method	LR	GPT-2 Small		GPT-2 Medium		GPT-2 Large		GPT-2 XL	
		Train	Val	Train	Val	Train	Val	Train	Val
Muon	$6 \times 10^{-4}$	25.46%	21.57%	22.10%	23.34%	28.56%	24.71%	27.32%	28.24%
AdaMuon		34.25%	33.73%	30.63%	31.96%	37.33%	31.34%	35.82%	31.04%
Muon	$1 \times 10^{-3}$	27.65%	25.46%	34.11%	35.26%	42.14%	35.87%	49.60%	43.72%
AdaMuon		37.33%	38.81%	40.07%	39.84%	48.32%	42.22%	51.76%	46.36%

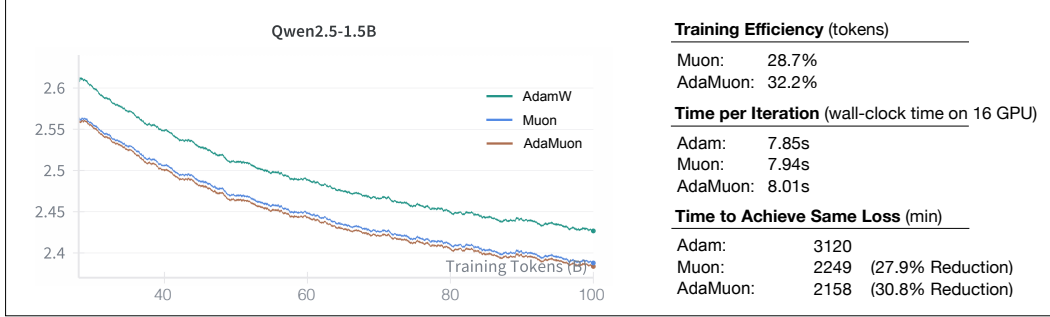


Figure 2: Results of AdamW, Muon, and AdaMuon when training Qwen2.5-1.5B dense model.

Table 2: Evaluation of Qwen2.5-1.5B trained by AdamW, Muon and AdaMuon. Abbreviations: ARC-C = ARC-Challenge, WinoG = WinoGrande, ComQA = CommonsenseQA.

Optimizer	MMLU	MMLU-Pro	TriviQA	ARC-C	GPQA	OBQA	HellaSwag	WinoG
	5-shot	5-shot	5-shot	25-shot	5-shot	5-shot	10-shot	5-shot
AdamW	30.67	5.14	20.96	24.40	19.70	37.80	47.69	54.38
Muon	<b>31.05</b>	5.43	<b>23.71</b>	<b>31.96</b>	22.22	37.90	47.85	<b>56.27</b>
AdaMuon	30.70	<b>6.43</b>	23.51	29.90	<b>26.77</b>	<b>39.70</b>	<b>49.68</b>	55.88
Optimizer	PIQA	ComQA	CHID	CMMLU	CEval	MBPP	GSM8k	Avg.
	5-shot	7-shot	5-shot	5-shot	5-shot	3-shot	4-shot	
AdamW	71.16	22.28	43.96	<b>29.34</b>	<b>31.30</b>	4.80	2.88	29.76
Muon	<b>72.20</b>	26.13	50.55	28.76	29.97	6.00	4.02	31.60
AdaMuon	71.38	<b>28.01</b>	<b>54.70</b>	28.93	31.10	<b>8.20</b>	<b>4.70</b>	<b>32.64</b>

trained with AdaMuon consistently outperform those trained with Muon and Adam across all evaluation metrics, further confirming the effectiveness of our approach in both convergence efficiency and final task performance.

## 5 CONCLUSION

This work presented AdaMuon, a new optimization paradigm that unifies the geometry-aware stability of Muon with the coordinate-wise adaptivity of variance-based scaling. By integrating a sign-stabilized orthogonal update, an element-wise second momentum estimator, and an RMS-aligned rescaling strategy, AdaMuon achieves both well-conditioned matrix-level updates and robust coordinate-wise adaptation—bridging the gap between efficiency and robustness in large-scale model training. Extensive experiments on GPT-2 and Qwen2.5 across multiple scales demonstrate that AdaMuon delivers consistent improvements over Adam and Muon, achieving up to **40%** gains in training efficiency with even superior final performance.

Looking forward, as model sizes and training demands continue to escalate, AdaMuon represents a promising step toward the next generation of optimizers that can scale efficiently while preserving

stability in increasingly complex optimization landscapes. At the same time, we close with an open question to the community: how far are we from realizing a truly practical and scalable second-order optimizer for modern large-scale deep learning?

## REFERENCES

- Jeremy Bernstein and Laker Newhouse. Old optimizer, new norm: An anthology. *arXiv preprint arXiv:2409.20325*, 2024.
- Tom Brown, Benjamin Mann, Nick Ryder, Melanie Subbiah, Jared D Kaplan, Prafulla Dhariwal, Arvind Neelakantan, Pranav Shyam, Girish Sastry, Amanda Askell, et al. Language models are few-shot learners. *Advances in neural information processing systems*, 33:1877–1901, 2020.
- Lizhang Chen, Jonathan Li, and Qiang Liu. Muon optimizes under spectral norm constraints. *arXiv preprint arXiv:2506.15054*, 2025.
- Aakanksha Chowdhery, Sharan Narang, Jacob Devlin, Maarten Bosma, Gaurav Mishra, Adam Roberts, Paul Barham, Hyung Won Chung, Charles Sutton, Sebastian Gehrmann, et al. Palm: Scaling language modeling with pathways. *Journal of Machine Learning Research*, 24(240): 1–113, 2023.
- John Duchi, Elad Hazan, and Yoram Singer. Adaptive subgradient methods for online learning and stochastic optimization. *Journal of machine learning research*, 12(7), 2011.
- Aaron Gokaslan, Vanya Cohen, Ellie Pavlick, and Stefanie Tellex. Openwebtext corpus, 2019.
- Vineet Gupta, Tomer Koren, and Yoram Singer. Shampoo: Preconditioned stochastic tensor optimization. In *International Conference on Machine Learning*, pp. 1842–1850. PMLR, 2018.
- Keller Jordan, Yuchen Jin, Vlado Boza, Jiacheng You, Franz Cesista, Laker Newhouse, and Jeremy Bernstein. Muon: An optimizer for hidden layers in neural networks, 2024. URL <https://kellerjordan.github.io/posts/muon/>.
- A Karpathy. Nanogpt, 2022. URL <https://github.com/karpathy/nanoGPT>.
- Diederik P Kingma and Jimmy Ba. Adam: A method for stochastic optimization. *arXiv preprint arXiv:1412.6980*, 2014.
- Aixin Liu, Bei Feng, Bing Xue, Bingxuan Wang, Bochao Wu, Chengda Lu, Chenggang Zhao, Chengqi Deng, Chenyu Zhang, Chong Ruan, et al. Deepseek-v3 technical report. *arXiv preprint arXiv:2412.19437*, 2024.
- Jingyuan Liu, Jianlin Su, Xingcheng Yao, Zhejun Jiang, Guokun Lai, Yulun Du, Yidao Qin, Weixin Xu, Enzhe Lu, Junjie Yan, et al. Muon is scalable for llm training. *arXiv preprint arXiv:2502.16982*, 2025.
- Ilya Loshchilov and Frank Hutter. Decoupled weight decay regularization. *arXiv preprint arXiv:1711.05101*, 2017.
- Team Moonshot. Kimi-k2, 2025. URL <https://moonshotai.github.io/Kimi-K2/>.
- Qwen, :, An Yang, Baosong Yang, Beichen Zhang, Binyuan Hui, Bo Zheng, Bowen Yu, Chengyuan Li, Dayiheng Liu, Fei Huang, Haoran Wei, Huan Lin, Jian Yang, Jianhong Tu, Jianwei Zhang, Jianxin Yang, Jiaxi Yang, Jingren Zhou, Junyang Lin, Kai Dang, Keming Lu, Keqin Bao, Kexin Yang, Le Yu, Mei Li, Mingfeng Xue, Pei Zhang, Qin Zhu, Rui Men, Runji Lin, Tianhao Li, Tianyi Tang, Tingyu Xia, Xingzhang Ren, Xuancheng Ren, Yang Fan, Yang Su, Yichang Zhang, Yu Wan, Yuqiong Liu, Zeyu Cui, Zhenru Zhang, and Zihan Qiu. Qwen2.5 technical report, 2025. URL <https://arxiv.org/abs/2412.15115>.
- Alec Radford, Jeffrey Wu, Rewon Child, David Luan, Dario Amodei, Ilya Sutskever, et al. Language models are unsupervised multitask learners. *OpenAI blog*, 1(8):9, 2019.



Ishaan Shah, Anthony M Polloreno, Karl Stratos, Philip Monk, Adarsh Chaluvvaraju, Andrew Hojel, Andrew Ma, Anil Thomas, Ashish Tanwer, Darsh J Shah, et al. Practical efficiency of muon for pretraining. *arXiv preprint arXiv:2505.02222*, 2025.

Jianlin Su, Murtadha Ahmed, Yu Lu, Shengfeng Pan, Wen Bo, and Yunfeng Liu. Roformer: Enhanced transformer with rotary position embedding. *Neurocomputing*, 568:127063, 2024.

Tijmen Tieleman. Lecture 6.5-rmsprop: Divide the gradient by a running average of its recent magnitude. *COURSERA: Neural networks for machine learning*, 4(2):26, 2012.

Hugo Touvron, Thibaut Lavril, Gautier Izacard, Xavier Martinet, Marie-Anne Lachaux, Timothée Lacroix, Baptiste Rozière, Naman Goyal, Eric Hambro, Faisal Azhar, et al. Llama: Open and efficient foundation language models. *arXiv preprint arXiv:2302.13971*, 2023.

Amund Tveit, Bjørn Remseth, and Arve Skogvold. Muon optimizer accelerates grokking. *arXiv preprint arXiv:2504.16041*, 2025.

Aohan Zeng, Xin Lv, Qinkai Zheng, Zhenyu Hou, Bin Chen, Chengxing Xie, Cunxiang Wang, Da Yin, Hao Zeng, Jiajie Zhang, et al. Glm-4.5: Agentic, reasoning, and coding (arc) foundation models. *arXiv preprint arXiv:2508.06471*, 2025.

## A PROOF OF THEOREM 1

**Proof.** From Condition (2) and (3),  $f$  must preserve orientation while being odd, hence  $f(x)$  takes the same sign as  $x$  and satisfies  $f(-x) = -f(x)$ . This constrains  $f$  to functions of the form  $f(x) = h(|x|) \cdot \text{sign}(x)$  with  $h : [0, \infty) \rightarrow [0, \infty)$ . From (1), for any  $c > 0$ ,  $h(c|x|) = h(|x|)$ . Thus,  $h$  is constant on  $(0, \infty)$ , i.e.  $h(r) = \kappa$  for all  $r > 0$ . From (4),  $\kappa$  must be finite. Therefore  $f(x) = \kappa \cdot \text{sign}(x)$ .

Finally, since  $g$  is globally scale-invariant ( $g(c\mathbf{M}_t) = g(\mathbf{M}_t)$ ), the multiplicative factor  $\kappa$  vanishes in effect. Hence the canonical representative is  $f(x) = \text{sign}(x)$ .

## B RATIONALE FOR OMITTING BIAS CORRECTION IN ADAMUON’S SECOND MOMENTUM

Unlike Adam, AdaMuon does not perform bias correction on its second-momentum estimation  $\mathbf{V}_t$  (line 8 in Algorithm 1). In Adam, the variance estimate is

$$\mathbf{V}_t = \beta \mathbf{V}_{t-1} + (1 - \beta) \mathbf{O}_t \odot \mathbf{O}_t, \quad (10)$$

which underestimates the true variance in early iterations. This bias must be corrected via

$$\hat{\mathbf{V}}_t = \frac{\mathbf{V}_t}{1 - \beta^t} \quad (11)$$

to avoid shrinking the step size excessively. In AdaMuon, however, the variance-adaptive update

$$\hat{\mathbf{O}}_t = \frac{\mathbf{O}_t}{\sqrt{\mathbf{V}_t} + \varepsilon} \quad (12)$$

is immediately followed by an RMS alignment step

$$\tilde{\mathbf{O}}_t = \gamma \hat{\mathbf{O}}_t, \quad \gamma = \frac{0.2 \cdot \sqrt{mn}}{\|\hat{\mathbf{O}}_t\|_F}, \quad (13)$$

which rescales the update to match a fixed target RMS magnitude (here, 0.2, matching Adam’s typical update norm). If  $\mathbf{V}_t$  is biased by a constant factor  $c$  (i.e.,  $\mathbf{V}_t \approx c \cdot \mathbf{V}_t^{\text{original}}$ ), then

$$\hat{\mathbf{O}}_t \propto \frac{1}{\sqrt{c}}, \quad \gamma \propto \sqrt{c}, \quad (14)$$

and the scaling factor  $\gamma$  cancels the bias exactly. Thus, the RMS-alignment step inherently removes any constant multiplicative bias in  $\mathbf{V}_t$ , making explicit bias correction unnecessary while keeping the update magnitude consistent with Adam.

By the way, AdaMuon does not apply bias correction to its first-momentum buffer  $\mathbf{M}_t$ . Any constant multiplicative factor  $c$  in  $\mathbf{M}_t$  has no effect on the normalized direction, because

$$\text{polar}(c \mathbf{M}_t) = \text{polar}(\mathbf{M}_t). \quad (15)$$

Thus, bias in the magnitude of  $\mathbf{M}_t$  is inherently removed by the orthogonalization step, making explicit first-momentum bias correction unnecessary.